

A Comparative Study of Infrared Asteroid Surveys: IRAS, AKARI, and WISE

Fumihiko Usui¹, Sunao Hasegawa², Masateru Ishiguro³, Thomas G. Müller⁴, and Takafumi Ootsubo⁵,

¹*Department of Astronomy, Graduate School of Science, The University of Tokyo, 7-3-1 Hongo, Bunkyo-ku, Tokyo 113-0033*
usui@astron.s.u-tokyo.ac.jp

²*Institute of Space and Astronautical Science, Japan Aerospace Exploration Agency, 3-1-1 Yoshinodai, Chuo-ku, Sagami-hara 252-5210*

³*Department of Physics and Astronomy, Seoul National University, San 56-1, Shillim-dong Gwanak-gu, Seoul 151-742, South Korea*

⁴*Max-Planck-Institut für Extraterrestrische Physik, Giessenbachstraße, 85748 Garching, Germany*

⁵*Astronomical Institute, Tohoku University, 6-3 Aoba, Aramaki, Aoba-ku, Sendai 980-8578*

(Received ; accepted)

Abstract

We present a comparative study of three infrared asteroid surveys based on the size and albedo data from the Infrared Astronomical Satellite (IRAS), the Japanese infrared satellite AKARI, and the Wide-field Infrared Survey Explorer (WISE). Our study showed that: (i) the total number of asteroids detected with diameter and albedo information with these three surveyors is 138,285, which is largely contributed by WISE; (ii) the diameters and albedos measured by the three surveyors for 1,993 commonly detected asteroids are in good agreement, and within $\pm 10\%$ in diameter and $\pm 22\%$ in albedo at 1σ deviation level. It is true that WISE offers size and albedo of a large fraction ($> 20\%$) of known asteroids down to a few km bodies, but we would suggest that the IRAS and AKARI catalogs compensate for larger asteroids up to several hundred km, especially in the main belt region. We discuss the complementarity of these three catalogs in order to facilitate the use of these data sets for characterizing the physical properties of minor planets.

Key words: catalogs — infrared: planetary systems — minor planets, asteroids: general — space vehicles — surveys

1. Introduction

Presently, the number of asteroids is known to be more than 620,000. Most asteroids are, however, known only from their orbital data and their other properties are poorly constrained. In particular, size of asteroid, which is one of the most basic physical quantities, has been unknown for most asteroids. Several techniques have been developed to determine the size of asteroid. One of the most effective methods for measuring asteroidal size and albedo indirectly is through the use of radiometry, where a combination of the thermal infrared flux and the absolute magnitude as the reflected sunlight. This radiometric method can provide unique data for asteroidal size and albedo. Observations in mid-infrared wavelengths are suitable for studying asteroids with this method, particularly in the inner solar system inside the orbit of Jupiter. Using radiometric measurements, a large number of objects can be observed in a short period of time, providing coherent data for large populations of asteroids within the asteroid belt.

Infrared observations can be made still better under ideal circumstances, from space. The first space-borne infrared telescope is the Infrared Astronomical Satellite (IRAS; Neugebauer et al. 1984), launched in 1983 and performed a survey of the entire sky. To date, there are two other infrared astronomical satellites dedicated to all-sky surveys: the Japanese infrared satellite AKARI (Murakami et al. 2007), and the Wide-field Infrared Survey Explorer (WISE; Wright et al. 2010). Other space-borne infrared telescopes, e.g., the Midcourse Space Experiment (MSX; Mill et al. 1994), the Infrared Space Observatory (ISO; Kessler et al. 1996), the Spitzer Space Telescope (Werner et al. 2004), and the Herschel Space Observatory (Pilbratt et al. 2010) have conducted a series of observations with imaging and/or spectroscopy of asteroids. Based on the all-sky survey data obtained by IRAS, AKARI, and WISE (hereafter I–A–W), the largest asteroid catalogs containing the size and albedo data were constructed. However, at present little is known about the consistency of these three catalogs of asteroidal data. Performance of the on-board detectors and the survey strategies are different, the time and season of the observations and the duration of surveys are different, and the thermal model of asteroids adopted for determining size and albedo are different, between I–A–W. The relationship between these three catalogs should be checked in order to facilitate the use of these data sets for scientific purposes.

In this paper, we compare the asteroidal catalog data obtained by I–A–W to investigate the consistency and characteristics of these data sets and reveal some benefits of the usage of synthesized these three data for studying the physical properties of minor planets. We have reviewed each surveyor and its data set, and have compiled these data into a single data set. Subsequently, we compare the number and distribution of the asteroids detected by these satellites, and discuss the completeness of the data sets obtained from each of the three satellites.

2. Size and albedo data set

2.1. Infrared all-sky surveyors: IRAS, AKARI, and WISE

In this paper the results obtained by IRAS, AKARI, and WISE (I–A–W) are used. Technical specifications of these three satellites are summarized in table 1.

A pioneering systematic asteroid survey with a space-borne telescope was made by IRAS in 1983. IRAS performed a survey of the entire sky with a 57 cm aperture telescope in ten months. The IRAS asteroid catalog was provided by Tedesco et al. (2002) as the supplemental IRAS minor planet survey¹ (SIMPS). The SIMPS includes the averaged results for 2,470 asteroids, which is 2,228 asteroids with at least two accepted observations and 242 that only have a single accepted sighting in a single band, by using the Standard Thermal Model (STM; Lebofsky et al. 1986). These data were revised by Ryan & Woodward (2010), which used the Near-Earth Asteroid Thermal Model (NEATM; Harris 1998) to derive asteroidal sizes and albedos, and which applied stricter criteria, selecting only objects with reported fluxes in three or four band-passes, and compiled the sizes and albedos for 1,483 objects.

AKARI is a second-generation infrared all-sky surveyor following IRAS. AKARI conducted a 16-month survey in six wavelength bands from the mid- to far-infrared with a 68.5cm aperture telescope. From many images taken in the mid-infrared part of the All-Sky Survey with the Infrared Camera (IRC; Onaka et al. 2007) on board AKARI, the infrared signals from asteroids were extracted and the Asteroid Catalog Using AKARI² (AcuA) was constructed, which contains the size and albedo data for 5,120 asteroids (Usui et al. 2011). Additionally, from the slow-scan observations in the pointed observation mode of AKARI, a serendipitous asteroidal catalog was constructed (AcuA-ISS; Hasegawa et al. 2013), which includes data from 88 main belt asteroids.

The WISE satellite, launched in December of 2009, made a mapping of the whole sky in four bands in the near- to mid- infrared, with a 40 cm aperture telescope. While IRAS and AKARI conducted continuous scanning of the sky with horizontally aligned detector arrays along the attitude control of the satellites at a constant scan rate (IRAS: $3'855\text{ s}^{-1}$, AKARI: $3'6\text{ s}^{-1}$), WISE used a different approach. The payload of WISE included a cryogenic scan mirror driven in a sawtooth pattern to cancel the orbital motion of the satellite, and to freeze the line of sight during each 11 s exposure interval (actual exposure times were 7.7 s in 3.4 and 4.6 μm bands and 8.8 s in 12 and 22 μm bands; Schwalm et al. 2005; Cutri et al. 2013), which achieves its wide field-of-view and high sensitivity. WISE accomplished its four-band full cryogenic survey phase in seven months, and continued survey observations for about six months after its cryogenic tanks became empty. The WISE asteroid data set is the most recent and the largest asteroid catalog provided by an enhancement program called NEOWISE (Mainzer et al.

¹ <http://sbn.psi.edu/pds/resource/imps.html>

² <http://darts.jaxa.jp/ir/akari/catalogue/AcuA.html>

2011a). The sizes and albedos of asteroids measured with WISE are currently published as a series of papers: Masiero et al. (2011); Masiero et al. (2012) for the main belt asteroids, Mainzer et al. (2011d); Mainzer et al. (2012) for the near-Earth asteroids, Grav et al. (2011); Grav et al. (2012a) for the Jovian Trojans, Grav et al. (2012b) for the Hilda group, and Bauer et al. (2013) for the scattered disk objects and Centaur populations.

In total, there are 137,837 asteroids in the WISE data set with valid diameter and albedo information.

2.2. Comparison of IRAS, AKARI, and WISE data sets

Figure 1 shows the relationship between the number of asteroids detected with each of these surveyors in the form of a Venn diagram. The number of asteroids detected with any three satellites is 138,285, which is 22% of currently known asteroids with orbits, and all three satellites detected a common 1,993 asteroids. Most objects were only detected with WISE, because WISE is about two orders of magnitude more sensitive than IRAS or AKARI at mid-infrared wavelengths (table 1). Nevertheless, 448 asteroids were detected with only AKARI and/or IRAS.

Figure 2 shows the distribution of the absolute magnitude for all asteroids detected by I–A–W with known orbits and semimajor axes smaller than 6 AU. This figure can be interpreted as reflecting the completeness of detections of known asteroids with the size and albedo data by three satellites. The AKARI asteroid catalog, which was constructed based on 16 months of the All-Sky Survey data, provides a 100% complete data set of all asteroids brighter than absolute magnitude of $H < 9$, which includes 40 km size asteroids at minimum (and all main belt asteroids brighter than $H < 10.3$, corresponding to 20 km or larger objects; Usui et al. 2013). It is important to include the entire population of asteroids with $H < 9$ for investigating the mass distribution of asteroids: asteroids with $H < 9$ account for more than 90% of the total mass of all asteroids. While WISE detected much smaller asteroids that peaked at $H \sim 15$, with corresponding diameter $d \geq 1.5$ km, some larger (and/or brighter) objects were not detected. It is notable that the numbers of undetected asteroids that were brighter than $H < 9$ are 23 for IRAS, 1 for AKARI, and 33 for WISE, which are very small proportion of the total number of objects detected by each satellite. There is only one asteroids with $H < 9$ that do not have measurements of its size and albedo so far: 1927 LA ($H = 8.81$). This belongs to the outer main belt asteroids and has an expected size of $d = 77$ km, assuming albedo of $p_v = 0.09$. The discovery of 1927 LA was reported in 1927 by Albrecht Kahrstedt at the Heidelberg-Königstuhl Observatory, Germany, but it was a single-apparition with only three observations, and one of them was noted as being in question (refer to *Astronomische Nachrichten* 232, 257 (1928) and also to the Minor Planet Center). No further follow-up observation has identified 1927 LA since these studies and, as such, we consider its existence is doubtful at present.

Figure 3 illustrates the distribution of asteroids identified by I–A–W as a function of

size and albedo. The size distribution in figure 3 (a) shows diameter maxima at ca. $d = 25$ km, 14 km, and 3 km for IRAS, AKARI, and WISE, respectively. This suggests that asteroids larger than these limits are almost always detected by each satellite, but that the completeness of the catalog for each satellite decreases rapidly for asteroids smaller than these values. The albedo distribution in figure 3 (b) exhibits a bimodal distribution: the primary peak is found around the geometric albedo of $p_v \sim 0.06$ for each data set; the secondary peaks are found at 0.16 for IRAS and AKARI, but at 0.25 for WISE. In these three data sets, there are extremely bright asteroids ($p_v > 0.5$), which are all smaller than 55 km, and mostly smaller than 10 km, in the main belt as well as the near-Earth region. The numbers of these anomalously high-albedo objects are, 5 in the IRAS catalog (0.20% of its total), 24 in the AKARI (0.46%), and 888 in the WISE (0.64%). It should be noticed that brighter high-albedo objects are more likely to be discovered, identified, and photometrically measured in visible wavelengths, especially toward smaller sized objects; in other words, the significant observational biases and selection effects still exist against darker and smaller objects. In contrast, infrared surveys are less biased against low albedo objects (e.g., Mainzer et al. 2011a).

Figure 4 and 5 show comparison of the sizes and albedos of the 1,993 asteroids commonly detected by I–A–W. Comparisons between IRAS and AKARI, and between IRAS and WISE have been studied (Usui et al. 2011; Mainzer et al. 2011c). From these figures, it is evident that the size and albedo measurements by all three satellites are in good agreement, although there are some systematic differences. In particular, the diameters estimated by AKARI are larger than those by IRAS but smaller than those by WISE. Therefore, of these three data sets, WISE yields the largest estimation of size, followed in order by AKARI and IRAS. Conversely, IRAS yields the highest albedo, and WISE the smallest albedo. This inverse relationship between size and albedo is unsurprising given that size is inversely proportional to the square root of albedo for a given absolute magnitude (e.g., Fowler & Chillemi 1992; Pravec & Harris 2007) as:

$$d = \frac{1329}{\sqrt{p_v}} 10^{-H/5} , \quad (1)$$

where d , p_v , and H are the diameter in units of km, the geometric albedo, and the absolute magnitude, respectively.

Figure 6 shows the distribution of the deviation of the sizes and albedos measured with I–A–W, from the respective mean values of those three data sets for the 1,993 commonly detected asteroids. The best-fit Gaussian parameters for these distributions are listed in table 2. As a result, they are in good agreement within $\pm 10\%$ in diameter and $\pm 22\%$ in albedo at 1σ deviation level.

3. Discussion

3.1. Survey period of the infrared satellites

The survey period is one of the important factors for asteroid surveys in the infrared (see table 1). At least one year is required to survey all of the solar system bodies beyond a semimajor axis of 2 AU with the surveyor in a fixed solar elongation of 90° , while the inertial sky can be covered in half a year. The IRAS mission, which lasted ten months, surveyed approximately 96% of the sky covered with two or more hours-confirming scans (Neugebauer et al. 1984; Beichman et al. 1988). The All-Sky Survey conducted for 16 months by AKARI fully covered the main belt region, using a combination of 170 litres of super-fluid liquid helium and two sets of two-stage Stirling cycle mechanical coolers (Nakagawa et al. 2007). Thus, the AKARI asteroid catalog provides a 100% complete data set of asteroids with $H < 9$, as mentioned above. The WISE mission conducted a seven-month-long full cryogenic survey and a six-month-long post-cryogenic survey (after depleting its cryogenic tanks). In the post-cryogenic phase, only the near-infrared channels (3.4 and 4.6 μm bands) were used. At these shorter wavelengths, asteroid fluxes are a mix of reflected sunlight and thermal emissions. Nevertheless, Mainzer et al. (2012), Masiero et al. (2012), and Grav et al. (2012a) produced reasonable estimates of the sizes and albedos of asteroids, assuming a relationship between visual albedo and infrared albedo, which are calibrated with data obtained in the full cryogenic phase.

3.2. Factors causing discrepancies among IRAS, AKARI, and WISE

The differences between the mean sizes and albedos obtained by I–A–W are generally within $\sim 10\%$ and $\sim 22\%$ of each other, respectively (at the 1σ standard deviation). These values are mostly larger than the uncertainties within each data set (typically, 5–13% for diameter and 10–33% for albedo). Several possible reasons may explain the I–A–W differences. First, the different types of measurements do not fully include system uncertainties. Also, several factors which may cause discrepancies originate from the physical properties of asteroids, such as their shape, thermal inertia, surface roughness, rotation rate, and pole orientation. Asteroids are often elongated and irregularly shaped, and sometimes form binary systems, which generate lightcurve variance as they rotate. The Asteroid Lightcurve Database³ (Warner et al. 2009) indicates that, as of September 2013, the mean value of the maximum amplitude of the lightcurve for the 5,730 available asteroids is 0.344 ± 0.296 mag. Asteroids with larger amplitude lightcurves are likely to add to the uncertainty in establishing their size and albedo, especially for estimations based on single or a few sightings.

In addition, uncertainties in the treatment of scattered sunlight in the visible wavelengths limit the accuracy of radiometric measurements. Usually, simultaneous observations in visible and infrared wavelengths are not achieved. Instead, the H – G system (Bowell et al. 1989) is

³ <http://www.minorplanet.info/lightcurvedatabase.html>

adopted to represent photometric values in visible wavelengths. Uncertainties in the absolute magnitudes mainly impact the accuracy of the resulting albedo values (Harris & Harris 1997). Pravec et al. (2012) found that a discrepancy exists between absolute magnitudes listed in the MPC orbit database and those measured by dedicated photometric observations over 30 years. They found that the MPC values are mostly too small for the 583 observed asteroids; the mean offset of H is -0.4 to -0.5 at $H \sim 14$. The slope parameter given in Pravec et al. (2012) varies from -0.15 to 0.55 (mean, 0.21 ± 0.09), while this value is often assumed to be 0.15 . These discrepancies can account for the uncertainties in the estimated albedo, especially for $H > 10$. Once improved measurements of H become available, the values for the sizes and albedos can be revised. For example, Harris & Harris (1997) devised a simple and convenient approximation for recalculating the size and albedo from improved H values that does not require detailed thermal model calculations.

Saturation of the observed flux leads to another severe problem for larger asteroids. Lebofsky (1989) found that the IRAS observations of (1) Ceres and (2) Pallas showed unusual behaviors (systematic wavelength variations) as compared with the results of ground-based observations, perhaps due to saturation in 25 and 60 μm bands. While these point sources may be saturated, properly corrected values do not affect estimates of the sizes of other objects using the IRAS data (Tedesco et al. 2002). Cutri et al. (2013) reported that point sources detected with WISE brighter than 0.88 Jy in 12 μm band or 12.0 Jy in 22 μm band show larger uncertainties owing to the onset of detector saturation. The former saturation level corresponds to the thermal emission from ~ 30 – 70 km sized main belt asteroids. In contrast, no sign of saturation is apparent in the AKARI observations (Ishihara et al. 2010); in 18 μm band, recorded flux densities for (1) Ceres were in the range of 500–800 Jy, and those for (4) Vesta were in the range of 470–600 Jy, both of which are below the saturation limit (D. Ishihara, 2014, private communication).

3.3. *The thermal model and the beaming parameter*

The STM (with some modification) or the NEATM can be used to characterize the physical properties of asteroids, although care should be exercised when applying these simple models to various types of asteroids. The STM produces good results if the asteroid has a small thermal inertia, rotates slowly, is observed at small solar phase angles, and is not heavily cratered or irregularly shaped (i.e., typical larger main belt asteroids). However, many asteroids are small irregular bodies with predominantly regolith-free rocky surfaces and relatively high thermal inertias (Delbó et al. 2007). Most studies support the assumption that asteroid surfaces are generally heavily cratered and rough at all scales (e.g., Ivanov et al. 2002). In combination with the lack of an atmosphere and small thermal skin depths, surface roughness gives rise to substantial temperature contrasts, even at small scales, and produces a *beaming effect* in which thermal emission is enhanced in the solar direction.

A beaming parameter was introduced to adjust the surface temperature by compensating for the angular distribution of the thermal emission (e.g., Lebofsky et al. 1986). The beaming parameter physically correlates with the surface roughness and thermal inertia of an asteroid, and in practice, it can be considered as a normalization or calibration factor. For the IRAS catalog, the STM was adopted as the thermal model, using a beaming parameter of $\eta = 0.756$, which was derived from observations of (1) Ceres and (2) Pallas using a ground-based telescope (Lebofsky et al. 1986). It should be noted that the size and albedo estimations of 60% of asteroids (and $> 80\%$ of asteroids larger than 40 km) detected by IRAS have been revised by a more robust estimation using the NEATM, with η values ranging from 0.75 to 2.75 (Ryan & Woodward 2010). The AKARI asteroid catalog was processed using the “modified” STM, in which η was determined separately for two observed mid-infrared bands ($\eta = 0.87$ for 9 μm band and 0.77 for 18 μm band), by comparing existing data from several different types of measurements for 55 asteroids ranging in diameter from 90 to 960 km (see Usui et al. 2011, table 11). The WISE results used the NEATM with independently varying η values, which were determined by fitting multiple observations using the WISE data alone; the results were then examined by comparisons with 49 unique objects with diameters ranging from 0.4 to 312 km (data from several sources; see Mainzer et al. 2011b, table 1). The distribution of η in the WISE thermal model is shown for main belt asteroids in, for example, figure 6 of Masiero et al. (2011) (the mean value of their beaming parameters is $\eta = 0.962 \pm 0.153$, for asteroid diameters of > 10 km).

Here, we consider the dependency of the size estimation on the value of the beaming parameter, under the conditions of the thermal model calculation. We assume an asteroid with given visible and thermal fluxes at given distances from the Sun and an observer. Once an incident solar flux is assumed, an absorbed flux is determined (although it depends weakly on albedo). A larger η causes lower surface temperatures of the thermal flux to balance the absorbed flux and the thermal emission. This can be easily found from the formulation of the temperature of the subsolar point (T_{ss}) on the surface of the asteroid (e.g., Harris 1998), as follows:

$$T_{\text{ss}} = \left\{ \frac{(1 - A_{\text{B}})S_{\text{s}}}{\eta\epsilon\sigma R_{\text{h}}^2} \right\}^{1/4}, \quad (2)$$

where A_{B} is the Bond albedo, S_{s} is the solar flux at 1 AU (i.e., the solar constant), η is the beaming parameter, ϵ is the infrared emissivity, σ is the Stefan–Boltzmann constant, and R_{h} is the heliocentric distance in units of AU. A lower temperature implies a lower thermal flux per unit area. To provide the observed thermal flux, a larger asteroid is needed, and a larger size is equivalent to a smaller albedo under a given flux in visible wavelengths. Thus, larger η values reflect larger sizes of asteroids.

It should also be noted that there is a phase angle (Sun–target–observer angle; α) dependency of the beaming parameter. In the STM, the temperature on the nightside of an asteroid

is assumed to be zero, which is a reasonable assumption at small phase angles, where the day-side flux dominates; i.e., in the case of the main belt asteroids. However, Harris & Lagerros (2002) pointed out that care must be exercised when applying simple thermal models to the near-Earth asteroids because thermal model calculations based on observations made at larger solar phase angles are subject to relatively large uncertainties; it was because of this that the NEATM was developed (Harris 1998). As compared with main belt asteroids, the near-Earth asteroids tend to have irregular shapes, and they are often observed at moderate to large solar phase angles ($\alpha > 30^\circ$), which is out of the valid range of the STM. If the nightside temperature is treated as non-zero, then the relationship between η and α can vary depending on the temperature distribution. Based on the WISE data obtained using the NEATM, the average relationship between η and α is given as $\eta = 0.00963^{\pm 0.00015}\alpha + 0.761^{\pm 0.009}$ (Mainzer et al. 2011d), or $\eta = 0.011^{\pm 0.001}\alpha + 0.79^{\pm 0.01}$ (Masiero et al. 2011), although the spread around this value is large for $0.3 \leq \eta \leq \pi$. Note that due to the constraints of the attitude control of infrared surveyors, the solar elongation angle of the WISE observations is fixed at approximately 90° , which means that the observing phase angle, heliocentric distance, and geocentric distance are strongly correlated.

The thermophysical model (TPM, Lagerros 1996; Lagerros 1997; Lagerros 1998), which is a sophisticated approach for asteroid modeling, assuming a spherical body, is developed to derive the size, albedo, thermal inertia, and sense of rotation without assuming a value of the beaming parameter. Müller et al. (2014) discussed the validity of the TPM for a selected target by using only this simple spherical shape model.

3.4. Comparisons with the other measurements

Importantly, none of the I–A–W catalogs consider the irregular shapes of asteroids. While a non-rotating spherical body is assumed for asteroids in both the STM and NEATM, the actual shapes of asteroids are generally elongated, especially in the cases of smaller asteroids. Figure 7 shows the relative differences between the diameters measured by I–A–W and the effective (volume-equivalent) diameters (D_{ref}) derived from the shape models determined by several methods: direct imaging with the Hubble Space Telescope (Tanga et al. 2003), with the adaptive optics system on the W.M. Keck II telescope (Hanuš et al. 2013; Marchis et al. 2006; Drummond et al. 2009; Conrad et al. 2007), or by spacecraft observations⁴(Thomas et al. 1996), stellar occultation combined with lightcurve inversion techniques (Ďurech et al. 2011), speckle interferometry (Cellino et al. 2003; Drummond et al. 1985), and radar observations (Ostro et al. 2000). In total, 88 main belt asteroids ranging in size from 30 to 540 km are included. The relative difference is defined as $(D_i - D_{\text{ref}})/D_{\text{ref}}$, where i refers to IRAS, AKARI, or WISE. The mean values of the relative differences are 2.8%, 1.7%, and 7.5% for IRAS, AKARI, and

⁴ Although more than ten asteroids have been explored by spacecraft flyby/rendezvous/landing/sample return, only (243) Ida ($d \sim 30$ km) has also been observed by all three infrared surveyors.

WISE, respectively, and the standard deviations for each are 12–13 %. We found that the size derived by AKARI is closer to that derived by IRAS or WISE. This is not a surprising result, as the beaming parameter adopted in the thermal model calculation in the AKARI catalog is calibrated with well-studied main belt asteroids larger than 90 km, whose size, shape, rotational properties, and albedo are known from different measurements, as mentioned above. In this respect, the diameters obtained by radiometric measurements based on I–A–W are reliable in a statistical sense, which are smoothed out and averaged over a limited number of observations, even though the sizes obtained by radiometric and other measurements can be discrepant by up to 30%.

4. Summary

A total of 138,285 asteroids were detected with three infrared all-sky surveyors: IRAS, AKARI, and WISE, which enabled their sizes and albedos to be determined by the radiometric method. IRAS made a pioneering asteroid survey including 2,470 objects. AKARI resulted in a 100% complete survey for larger asteroids ($H < 9$, corresponding 40 km or larger) in its 16-month mission. WISE has significantly improved the number of smaller sized asteroids detected ($H < 15$, corresponding 1.5 km or larger) as a result of its higher sensitivity compared with IRAS and AKARI. 1,993 asteroids were commonly detected by all three satellites, and the size and albedo measurements of these asteroids by each satellite are in good agreement (within $\pm 10\%$ for diameter and $\pm 22\%$ for albedo). The data sets from these three satellites complement one another and will provide an important database for statistical analysis of asteroid populations and characterizing the physical properties of each asteroid.

This study is based on observations with AKARI, a JAXA project with the participation of ESA. This work also makes use of data products from the Wide-field Infrared Survey Explorer, which is a joint project of the University of California, Los Angeles, and the Jet Propulsion Laboratory/California Institute of Technology, funded by the National Aeronautics and Space Administration. FU would like to thank Takao Nakagawa (ISAS/JAXA), Daisuke Ishihara (Nagoya University), and Takashi Onaka (the University of Tokyo), for their valuable comments. MI is supported by the National Research Foundation of Korea (NRF) grant funded by the Korea Government (MEST) (No. 2012R1A4A1028713). SH is supported by the Space Plasma Laboratory, ISAS/JAXA. TO is supported in part by JSPS KAKENHI Grant Number 25400220. We thank the anonymous referee for careful reading and providing constructive suggestions.

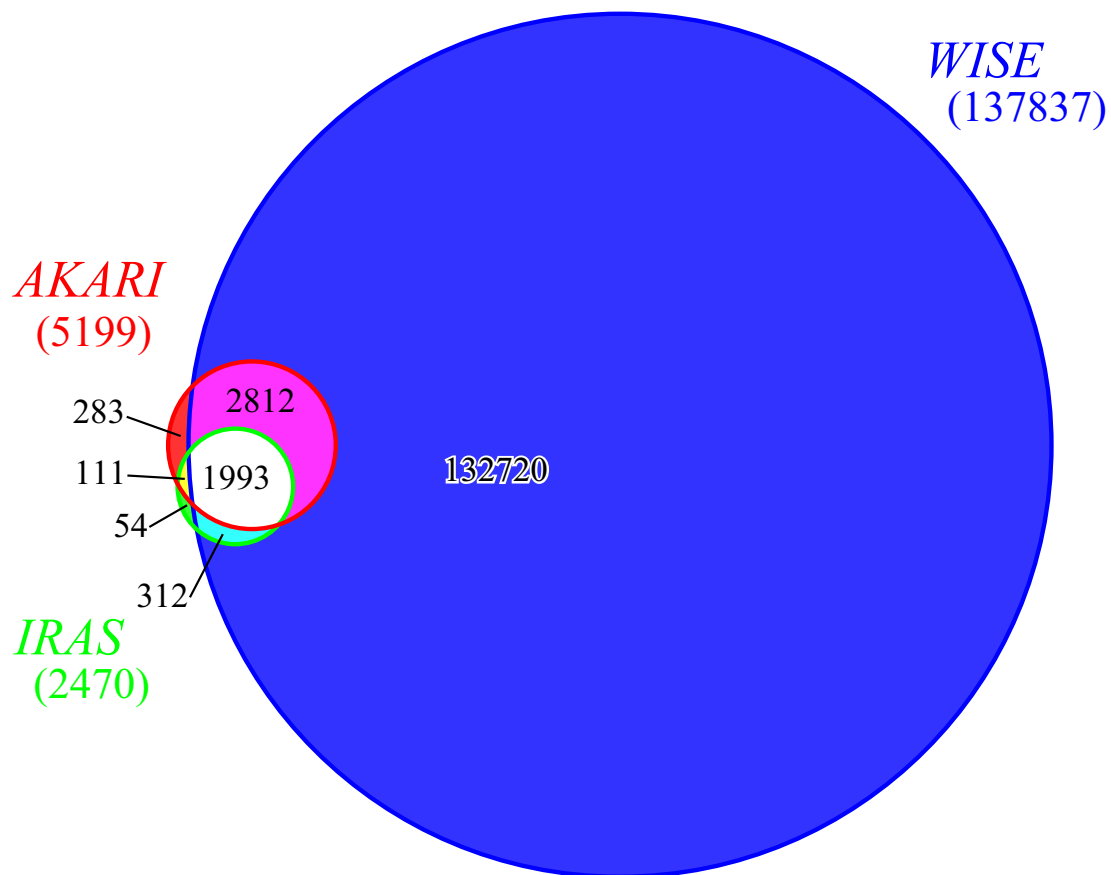


Fig. 1. A comparison of the number of asteroids detected with IRAS, AKARI, and WISE shown as a Venn diagram. The total number of asteroids detected with either IRAS, AKARI, or WISE is 138,285.

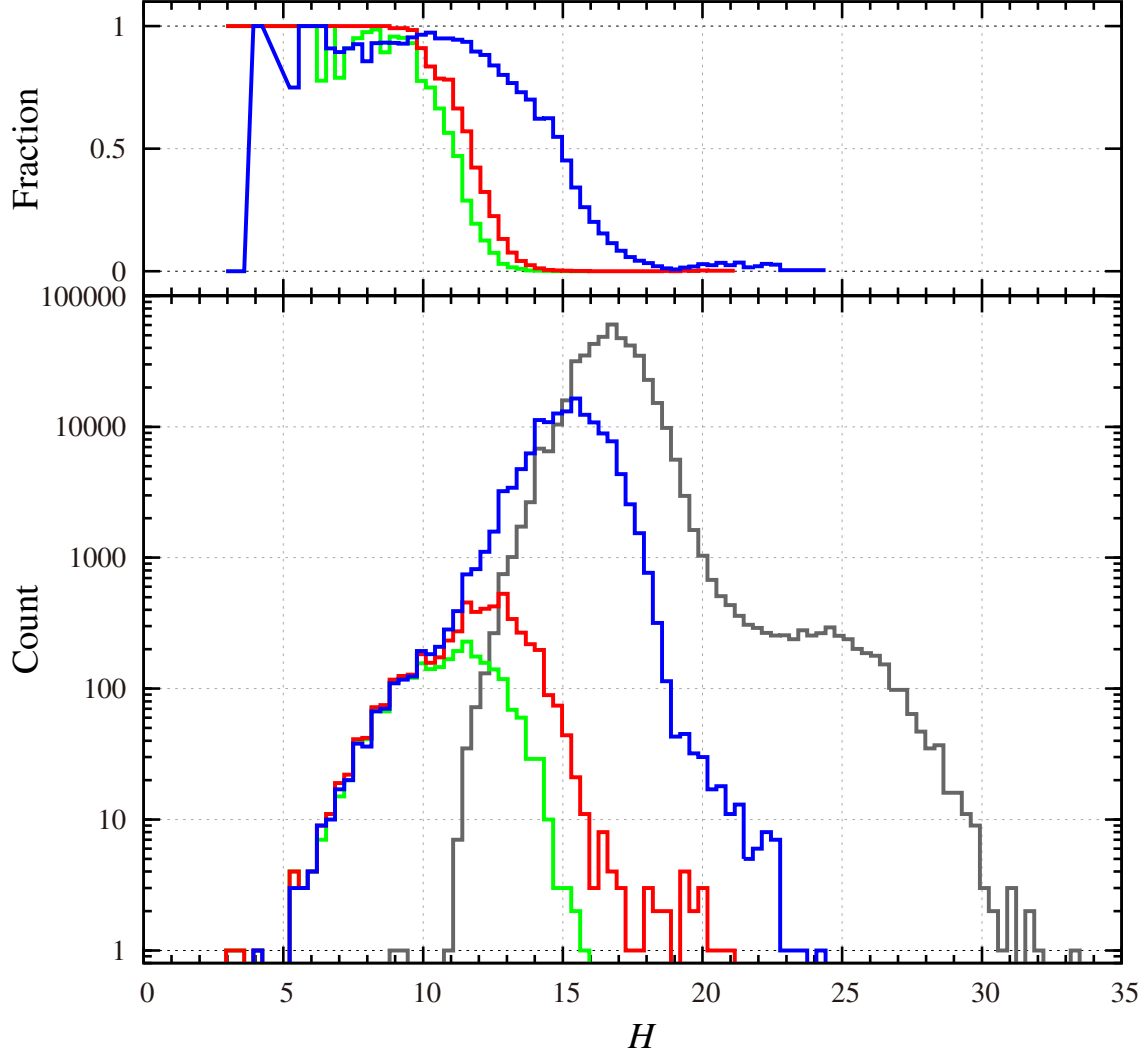


Fig. 2. Distribution of absolute magnitude (H) for asteroids detected with I-A-W, or undetected, with known orbits with semi-major axes smaller than 6 AU. The upper panel shows the fraction of detected asteroids of the total, and the lower panel shows the distribution of detected asteroids, by IRAS (green), AKARI (red), WISE (blue), and asteroids undetected by I-A-W (gray). Note that the absolute magnitude was not measured with these infrared surveyors, but determined by ground-based observational data in visible wavelengths (see, e.g., Bowell et al. 1994).

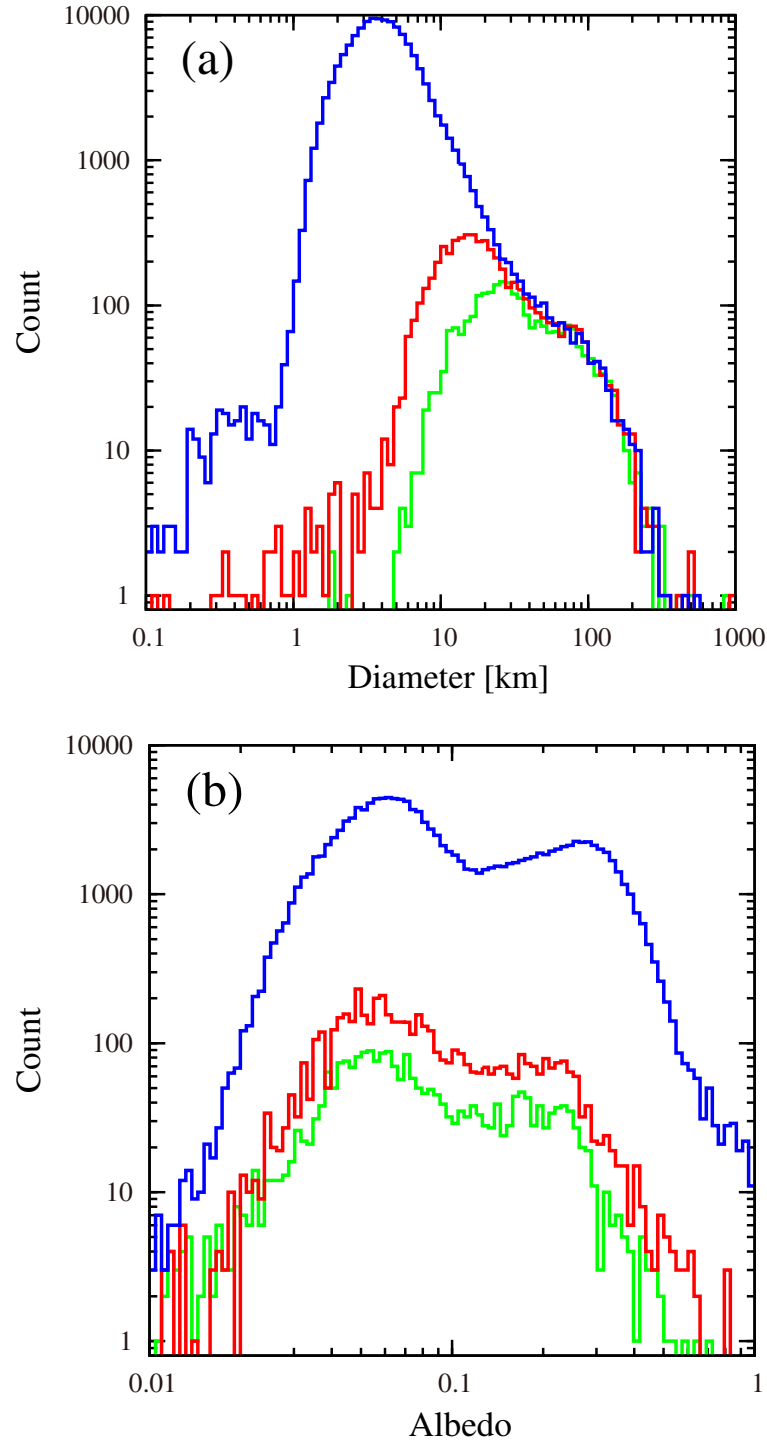


Fig. 3. Distribution of (a) diameter and (b) albedo of asteroids detected by IRAS (green), AKARI (red), and WISE (blue). The bin size is set at 100 segments for the range of 0.1 to 1000 km in the logarithmic scale for (a) and 100 segments for the range of 0.01 to 1.0 in the logarithmic scale for (b).

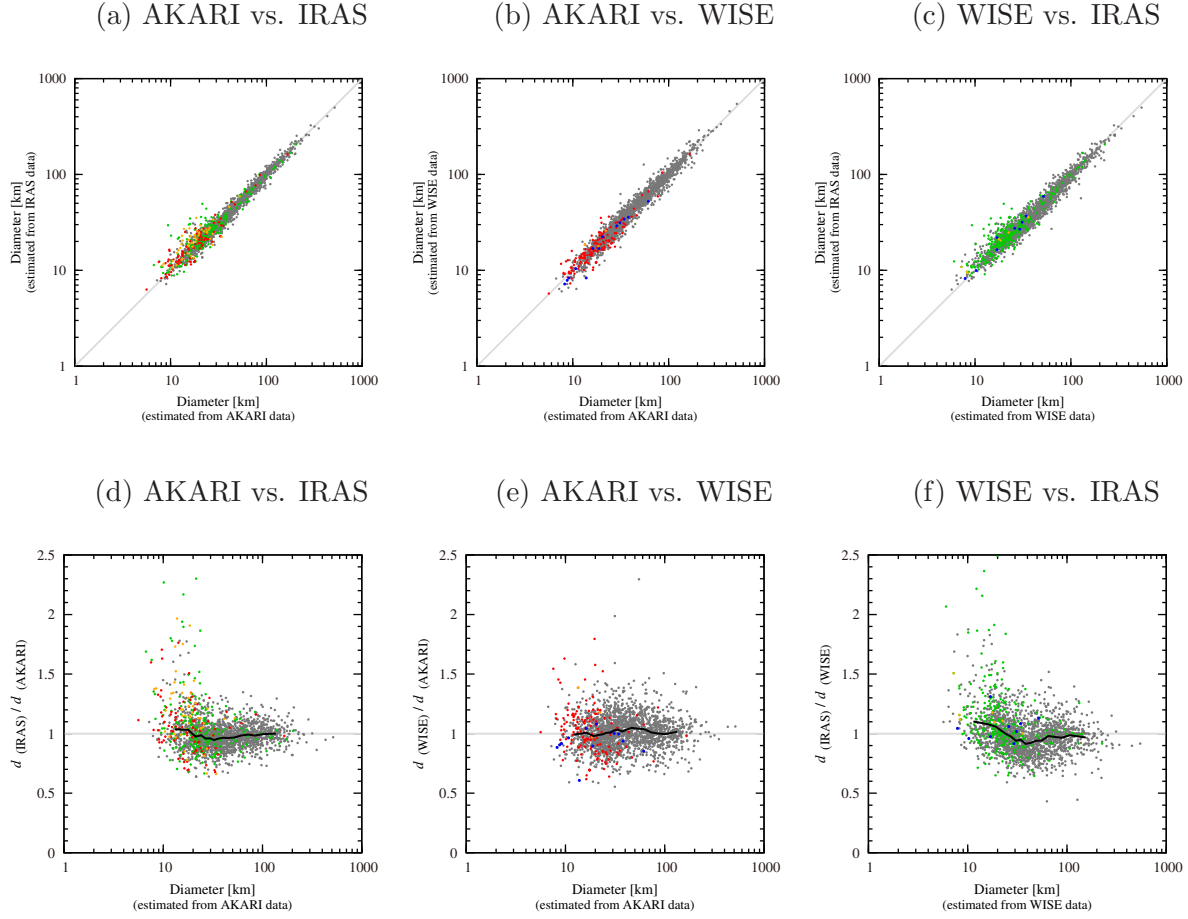


Fig. 4. A comparison of the differences in diameter obtained on the asteroids commonly detected by all three satellites, i.e., IRAS, AKARI, and WISE (1,993 asteroids). Green, red, and blue dots denote the asteroids observed with the single accepted sightings of IRAS (Tedesco et al. 2002), the single event detections of AKARI (Usui et al. 2011), and the single band detections of WISE (Masiero et al. 2011), respectively. Yellow dots denote the asteroids with the single observations in both satellites in each panel. Note that in the WISE data any objects with a single detection in a single band are not accepted (see, e.g., Mainzer et al. 2011a); the data with at least four time detections in a single band are included. Apart from these small number of detections, the mean values of the diameter ratios obtained by the different satellites are 0.982 (0.113), 1.013 (0.139), and 0.982 (0.154) for (d), (e), and (f), respectively, where the numbers in parentheses are the standard deviation (1σ). Thick black lines in the lower three panels show the running averages of the diameters for 100 object-wide bins, excluding the data corresponding to the small number of detections.

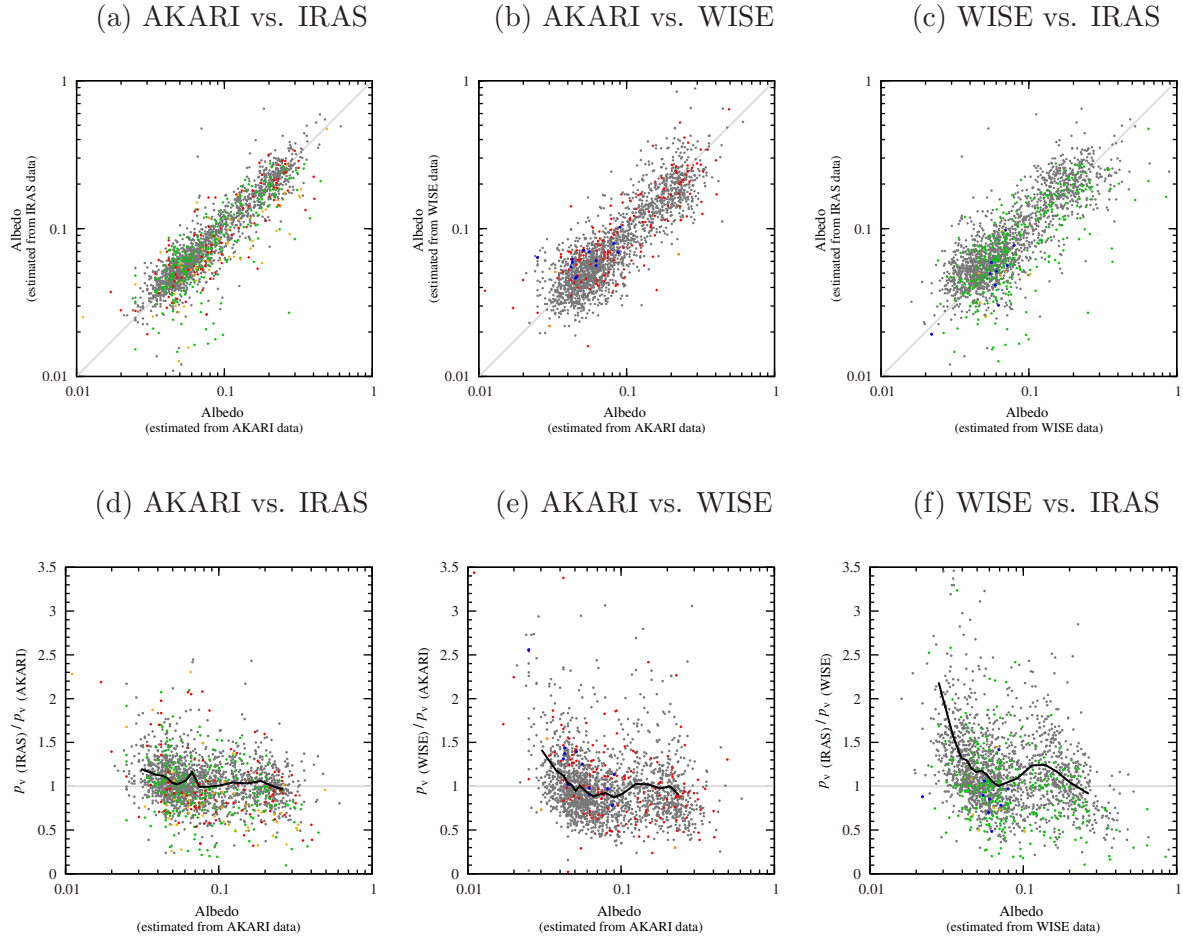


Fig. 5. Same as figure 4 but in albedo. Apart from the small number of detections, the mean values of the albedo ratios obtained by the different satellites are 1.057 (0.296), 0.986 (0.364), and 1.222 (1.216) for (d), (e), and (f), respectively, where the numbers in parentheses are the standard deviation (1σ).

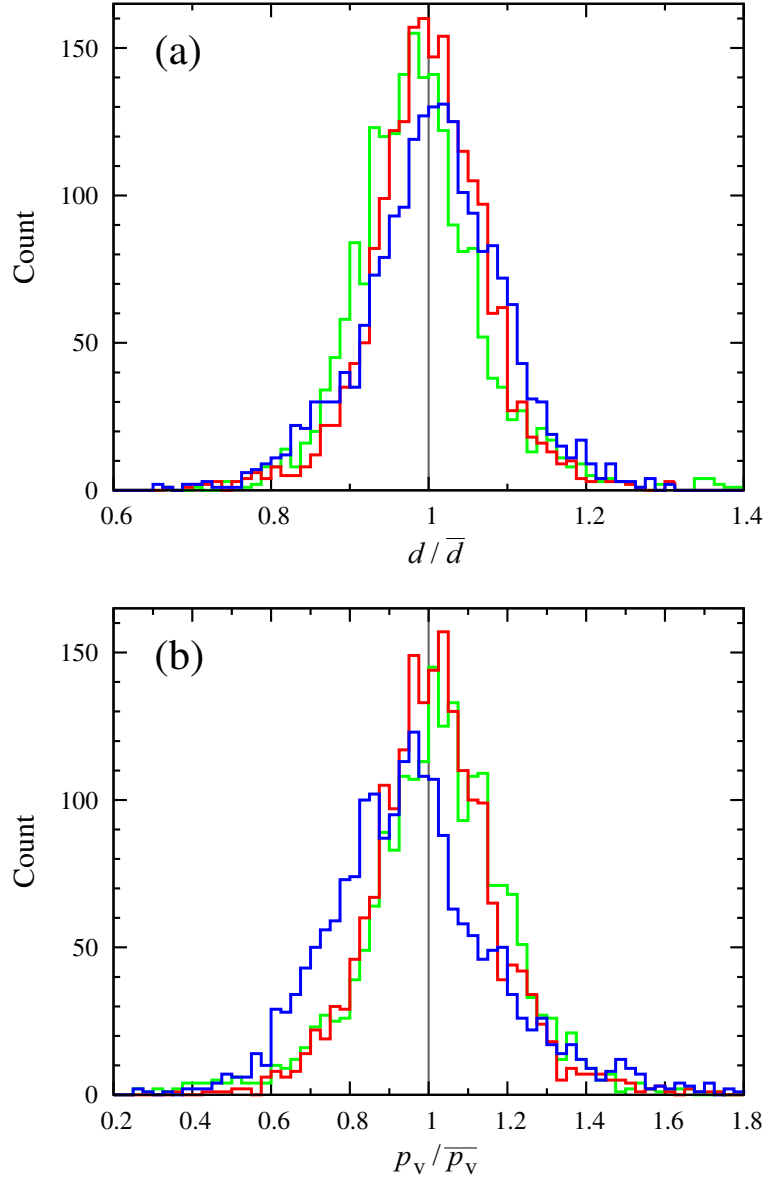


Fig. 6. The distribution of the deviation of diameter (d) and albedo (p_v) measured by IRAS (green), AKARI (red), or WISE (blue), from the mean values of the three satellites (\bar{d} , \bar{p}_v) for the 1,993 commonly detected asteroids. The means and standard deviations of the best-fitting Gaussian curves are summarized in table 2.

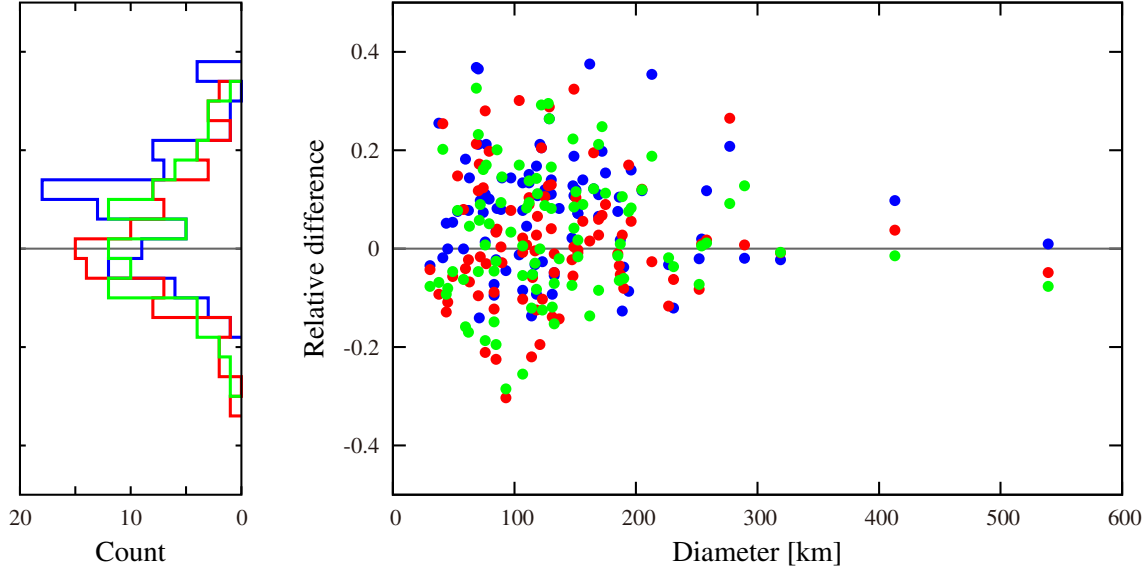


Fig. 7. Relative difference between effective diameters (D_{ref}) determined by direct imaging with HST or Keck AO, occultations, speckle interferometry, or radar (see text) and diameters derived by I–A–W. Here relative difference is defined as $(D_i - D_{\text{ref}})/D_{\text{ref}}$, where i refers to IRAS, AKARI, or WISE. Color dots mean the diameter measured by IRAS (green), AKARI (red), or WISE (blue).

Table 1. Details of the infrared all-sky survey satellites.

	IRAS ^a	AKARI ^b	WISE ^c
Size [m]	$3.6 \times 3.2 \times 2.1$	$5.5 \times 1.9 \times 3.7$	$2.9 \times 2.0 \times 1.7$
Weight [kg]	1083	952	750
Telescope	57cm, $f/9.56$ Ritchey-Chrétien	68.5cm, $f/6$ Ritchey-Chrétien	40cm, $f/3.375$ Mirror complex ^d
Cryogen	LHe (480 ℓ)	LHe (179 ℓ) with 2-stage Stirling coolers	Solid hydrogen (15.7 kg)
Altitude of orbit	900 km	750 km	525 km
Launch [UT]	1983/01/26 02:17:00	2006/02/21 21:28:00	2009/12/14 14:09:00
End of operation [UT]	1983/11/23	2011/11/24 08:23:00	2011/02/17 20:00:00 ^e
Period of survey ^f	1983/02/09–1983/11/22 287 days	2006/04/26–2007/08/26 488 days	2010/01/07–2010/08/05 211 days
Wavelengths [μm]	12,25,50,100	9,18,65,90,140,160 ^g	3.4,4.6,12,22
5 σ sensitivity [mJy]	350,330,430,1500 ^a	50,90 ^h ,3200,550,3800,7500 ⁱ	0.08,0.1,0.85,5.5 ^j
FOV ^k [°]	4.5~5.0	~10	47
Sky coverage	> 96%	> 96%	> 99%

(a)The Infrared Astronomical Satellite, Neugebauer et al. (1984); Beichman et al. (1988) (b)Murakami et al. (2007); pre-launch designation is ASTRO-F. Note that AKARI means “light” in Japanese and is not assigned a special acronym. (c)The Wide-field Infrared Survey Explorer, Wright et al. (2010); Cutri et al. (2013) (d)The optical sub-assembly of WISE consisted of an afocal telescope with six mirrors, a scan mirror, and imaging optics with six mirrors, which are required to cover wide field-of-view and have extremely low distortion for performing internal scanning without image blurring. It is a kind of “a Cassegrain-like objective” (Schwalm et al. 2005). (e)There is a report that WISE would be reactivated in September 2013. (f)Cryogenic cooled phase only. (g)While the all-sky survey with AKARI was measured in six bands, the asteroid catalog was constructed using two mid-infrared bands (9 and 18 μm). (h)Ishihara et al. (2010) (i)Yamamura et al. (2010) (j)Mainzer et al. (2011a) (k)In scan direction.

Table 2. Best-fit parameters of the Gaussian curve fitting for the size (d) and albedo (p_v) distributions in figure 6.

	\bar{d}	$\sigma(\bar{d})$	$\bar{p_v}$	$\sigma(\bar{p_v})$
IRAS	0.992	0.094	1.022	0.193
AKARI	1.001	0.076	1.016	0.164
WISE	1.006	0.093	0.962	0.222

References

- Bauer, J. M., et al. 2013, *ApJ*, 773, 22
- Beichman, C. A., Neugebauer, G., Habing, H. J., Clegg, P. E., & Chester, T. J. 1988, *Infrared astronomical satellite (IRAS) catalogs and atlases. Volume 1: Explanatory supplement*, 1
- Bowell, E., Hapke, B., Domingue, D., Lumme, K., Peltoniemi, J., & Harris, A. W. 1989, in *Asteroids II*, ed. R. P. Binzel et al. (Tucson: University of Arizona Press), 524
- Bowell, E., Muinonen, K., & Wasserman, L. H. 1994, in *Asteroids, Comets, Meteors 1993*, ed. A. Milani et al. (Dordrecht: Kluwer Academic Publishers), 477
- Cellino, A., Diolaiti, E., Ragazzoni, R., Hestroffer, D., Tanga, P., & Ghedina, A. 2003, *Icarus*, 162, 278
- Conrad, A. R., et al. 2007, *Icarus*, 191, 616
- Cutri, R. M., et al. 2013, *Explanatory Supplement to the WISE All-Sky Data Release Products*
<http://wise2.ipac.caltech.edu/docs/release/allsky/expsup/index.html>
- Delbó, M., Dell’Oro, A., Harris, A. W., Mottola, S., & Mueller, M. 2007, *Icarus*, 190, 236
- Drummond, J. D., Hege, E. K., Cocke, W. J., Freeman, J. D., Christou, J. C., & Binzel, R. P. 1985, *Icarus*, 61, 232
- Drummond, J., Christou, J., & Nelson, J. 2009, *Icarus*, 202, 147
- Ďurech, J., et al. 2011, *Icarus*, 214, 652
- Fowler, J. W., & Chillemi, J. R. 1992, *Phillips Lab. Tech. Rep.*, 2049, 17
- Grav, T., et al. 2011, *ApJ*, 742, 40
- Grav, T., et al. 2012a, *ApJ*, 744, 197
- Grav, T., Mainzer, A. K., Bauer, J. M., Masiero, J. R., & Nugent, C. R. 2012b, *ApJ*, 759, 49
- Hanuš, J., Marchis, F., & Ďurech, J. 2013, *Icarus*, 226, 1045
- Harris, A. W. 1998, *Icarus*, 131, 291
- Harris, A. W. and Harris, A. W. 1997, *Icarus*, 126, 450
- Harris, A. W., & Lagerros, J. S. V. 2002, in *Asteroids III*, ed. W. F. Bottke Jr. et al. (Tucson: University of Arizona Press), 205
- Hasegawa, S., Müller, T. G., Kuroda, D., Takita, S., & Usui, F. 2013, *PASJ*, 65, 34
- Ishihara, D., et al. 2010, *A&A*, 514, A1
- Ivanov, B. A., Neukum, G., Bottke, Jr., W. F., & Hartmann, W. K. 2002, in *Asteroids III*, ed. W. F. Bottke Jr. et al. (Tucson: University of Arizona Press), 89
- Kessler, M. F., et al. 1996, *A&A*, 315, L27
- Lagerros, J. S. V. 1996, *A&A*, 310, 1011
- Lagerros, J. S. V. 1997, *A&A*, 325, 1226
- Lagerros, J. S. V. 1998, *A&A*, 332, 1123
- Lebofsky, L. A., et al. 1986, *Icarus*, 68, 239
- Lebofsky, L. A. 1989, *Icarus*, 78, 355
- Mainzer, A., et al. 2011a, *ApJ*, 731, 53
- Mainzer, A., et al. 2011b, *ApJ*, 736, 100
- Mainzer, A., Grav, T., Masiero, J., Bauer, J., Wright, E., Cutri, R. M., Walker, R., & McMillan, R. S. 2011c, *ApJ*, 737, L9

- Mainzer, A., et al. 2011d, *ApJ*, 743, 156
- Mainzer, A., et al. 2012, *ApJ*, 760, L12
- Marchis, F., Kaasalainen, M., Hom, E. F. Y., Berthier, J., Enriquez, J., Hestroffer, D., Le Mignant, D., & de Pater, I. 2006, *Icarus*, 185, 39
- Masiero, J. R., et al. 2011, *ApJ*, 741, 68
- Masiero, J. R., Mainzer, A. K., Grav, T., Bauer, J. M., Cutri, R. M., Nugent, C., & Cabrera, M. S. 2012, *ApJ*, 759, L8
- Mill, J. D., et al. 1994, *J. Spacecr. Rockets*, 31, 900
- Müller, T. G., Hasegawa, S., Usui, F. 2014, *PASJ*, in this volume
- Murakami, H., et al. 2007, *PASJ*, 59, S369
- Nakagawa, T., et al. 2007, *PASJ*, 59, S377
- Neugebauer, G., et al. 1984, *ApJ*, 278, L1
- Onaka, T., et al. 2007, *PASJ*, 59, S401
- Ostro, S. J., et al. 2000, *Science*, 288, 836
- Pilbratt, G. L., et al. 2010, *A&A*, 518, L1
- Pravec, P., & Harris, A. W. 2007, *Icarus*, 190, 250
- Pravec, P., Harris, A. W., Kušnirák, P., Galád, A., & Hornoch, K. 2012, *Icarus*, 221, 365
- Ryan, E., & Woodward, C. 2010, *AJ*, 140, 933
- Schwalm, M., Barry, M., Perron, G., Sampath, D., LaMalva, F., Guregian, J., & Crowther, B. 2005, *Proc. SPIE*, 5904, 178
- Tanga, P., Hestroffer, D., Cellino, A., Lattanzi, M., Di Martino, M., & Zappalà, V. 2003, *A&A*, 401, 733
- Tedesco, E. F., Noah P. V., Noah, M., & Price, S. D. 2002, *AJ*, 123, 1056
- Thomas, P. C., Belton, M. J. S., Carcich, B., Chapman, C. R., Davies, M. E., Sullivan, R., & Veverka, J. 1996, *Icarus*, 120, 20
- Usui, F., et al. 2011, *PASJ*, 63, 1117
- Usui, F., Kasuga, T., Hasegawa, S., Ishiguro, M., Kuroda, D., Müller, T. G., Ootsubo, T., & Matsuhara, H. 2013, *ApJ*, 762, 56
- Warner, B. D., Harris, A. W., & Pravec, P. 2009, *Icarus*, 202, 134
- Werner, M. W., et al. 2004, *ApJS*, 154, 1
- Wright, E. L., et al. 2010, *ApJ*, 140, 1868
- Yamamura, I., Makiuti, S., Ikeda, N., Fukuda, Y., Oyabu, S., Koga, T., & White, G. J. 2010, *AKARI/FIS All-Sky Survey Bright Source Catalogue Version 1.0 Release Note*
http://www.ir.isas.jaxa.jp/AKARI/Observation/PSC/Public/RN/AKARI-FIS_BSC_V1_RN.pdf